The low-temperature specific heat of scandium

1993 J. Phys.: Condens. Matter 5 1721

(http://iopscience.iop.org/0953-8984/5/11/012)

J. Phys.: Condens. Matter 5 (1993) 1721–1732. Printed in the UK

The low-temperature specific heat of scandium

W Götz and H Winter

Institut für Nukleare Festkörperphysik, Kernforschungszentrum Karlsruhe, PO Box 3640, W-7500 Karlsruhe, Federal Republic of Germany

Received 17 November 1992

Abstract. We apply our first-principles SDFA-RPA scheme to calculate the spin fluctuation spectrum as well as the phonon and the spin fluctuation Eliashberg functions of the lightest rare earth metal scandium. These quantities are used to evaluate the low-temperature electron mass enhancement. We find that both terms are sizeable. Together with our calculated bandstructure densities of states at the Fermi energy, our results are compatible with experimental data for the low-temperature specific heat coefficient.

1. Introduction

Both the magnitude and the temperature dependence of the electronic specific heat coefficient, γ, of the lightest rare earth metal scandium exhibits features leading to the conclusion that many-body enhancement effects play an important role in this substance. Depending on the reference for the calculated bandstructure density of states, $n(\epsilon_F)$, at the Fermi energy, a whole range of values for the electron mass enhancement parameter, λ, have been deduced from specific heat measurements by using the relation $\lambda = \gamma/n(\epsilon_F) - 1$. Whilst the measurements of γ show little scatter (the numbers obtained by Tsang *et al* (1985) and Flotow and Osborne (1967) are 10.334 and 10.66 mJ mol^{-1} K^{-2} respectively), there is a considerable variance in the published values for $n(\epsilon_F)$. According to the work of Tsang *et al* (1985), who collect bandstructure data for Sc, the value for this quantity varies between 31.80 (Gopta and Freeman 1976) and 19.84 (Sen and Chatterjee 1980) states Ryd^{-1}/atom, giving rise to values for λ between 0.87 and 2.01. Even the lowest number in this spectrum cannot be explained by electron–phonon coupling alone. From an analysis of the measured temperature dependent specific heat, c_v, up to 600 K, Knapp and Jones (1972) estimate $\lambda_{phon} = 0.3$. Papaconstantopoulos *et al* (1977) calculated λ_{phon} within the rigid muffin tin approximation (RMTA) for electron–phonon coupling, obtaining $\lambda_{phon} = 0.639$. Since their $n(\epsilon_F) = 32.04$ leads to $\lambda = 0.860$, a sizeable additional contribution to λ must also be postulated within the frame of this theoretical treatment. It has been speculated for some time that coupling of the electrons to spin fluctuations might provide this extra term. The long-wavelength Stoner enhancement, S, of Sc, lying in the range of three to four, gives in fact a hint that the amplitudes of the spin fluctuations might be considerable in this substance. However, as our previous investigations on the elemental metals Pd and V (Stenzel *et al* 1988) show, $S(0)$ is not an appropriate measure for the magnitude of the electron–spin fluctuation mass enhancement, since fluctuations of all wavevectors within the

0953-8984/93/111721+12$07.50

Brillouin zone (BZ) contribute to this quantity. To assess λ_{spin}, it is necessary to calculate the dynamical spin fluctuation spectrum and the electron–spin fluctuation coupling function at relevant q points throughout the BZ.

While in previous work we treated magnetic resonance properties of scandium (Götz and Winter 1993), we concentrate in the present paper on the low-temperature electronic mass enhancement coefficient, λ, evaluating from first principles both its spin fluctuation part, λ_{spin}, and its phonon part, λ_{phon}, in the frame of the SDFA-RPA. In section 2 we sketch the formalism, and present the KKR bandstructure in section 3. Section 4 is devoted to the discussion of our results for the phonon and the spin fluctuation contributions to λ and we close with a summary in section 5.

2. Formalism

To start with the phononic part, λ_{phon} is determined by minus the first frequency moment of the Eliashberg function, $\alpha^2F(\omega)$, through the following relation:

$$\lambda_{phon} = 2\int_0^\infty d\omega \frac{\alpha^2F(\omega)}{\omega}. \tag{1}$$

To evaluate $\alpha^2F(\omega)$, we need to know the wavevector and frequency dependent phonon propagator $D^{\tau\tau'}_{\alpha\alpha'}(q,\omega)$, the electron–phonon coupling function $\pi_q(r,r')$, and the electron–phonon coupling potential $\delta V^\tau_\alpha(r)$. In terms of these quantities $\alpha^2F(\omega)$ is determined through the following equation:

$$\alpha^2F(\omega) = \int \frac{dq}{\Omega_{BZ}} \int_{\Omega_{unit}} dr \sum_{\alpha\alpha'} \int_{\Omega_{unit}} dr' \delta V^\tau_\alpha(r) D''^{\tau\tau'}_{\alpha\alpha'}(q,\omega) \delta V^{\tau'}_{\alpha'}(r') \pi_q(r,r'). \tag{2}$$

Here, the space integrals go over the volume of the unit cell and the integral over the wavevector q covers the BZ. The indices τ, τ' label the atoms in the unit cell.

In harmonic approximation $D^{\tau\tau'}_{\alpha\alpha'}(q,\omega)$ can be expressed by the phonon frequencies $\omega_{q\lambda}$ and the phonon polarization vectors $e_{q,\lambda}$. Its spectral function, D'', for positive frequencies reads:

$$D''^{\tau\tau'}_{\alpha\alpha'}(q,\omega) = \sum_\lambda \frac{\pi}{2\sqrt{M_\tau M_{\tau'}}\omega} \delta(\omega-\omega_{q,\lambda}) e^\tau_{q\lambda\alpha} e^{\tau'*}_{q,\lambda\alpha'} \exp[iq(\tau-\tau')]. \tag{3}$$

Using the local representation $r = (\rho,\tau,j)$ for the space coordinates the formula for π reads (Stenzel *et al* 1988):

$$\pi_q(\rho\tau,\rho'\tau') = \frac{2}{n(\epsilon_F)\pi^3} \sum_j [\mathrm{Im}\, g(\rho\tau,\rho'\tau' j;\epsilon_F)]^2 \exp(iqR_j)$$

$$= \sum_j \pi'(\rho\tau,\rho'\tau';j)\exp(iqR_j). \tag{4}$$

Here, the j sum goes over the unit cells of the crystal at positions R_j, g is the one-particle electron Green function in bandstructure approximation, and $n(\epsilon_F)$ is to be inserted in states Ryd^{-1}/unit cell.

In RMTA δV is given by

$$\delta V^\tau_\alpha(\rho) = (\rho_\alpha/\rho)\partial V^\tau(\rho)/\partial\rho \tag{5}$$

with $V^{\tau}(\rho)$ the crystalline muffin tin potential at site τ. Inserting equations (2) to (5) into equation (1), we finally obtain

$$\alpha^2 F(\omega) = \sum_{\tau\tau'} \int \frac{\mathrm{d}q}{\Omega_{\mathrm{BZ}}} \sum_{\alpha\alpha'} D^{\tau\tau'}_{\alpha\alpha'}{}''(q,\omega) \sum_j \int \mathrm{d}\rho \frac{\partial V^{\tau}(\rho)}{\partial \rho} \frac{\rho_\alpha}{\rho}$$

$$\times \int \mathrm{d}\rho' \frac{\partial V^{\tau'}(\rho')}{\partial \rho'} \frac{\rho'_{\alpha'}}{\rho'} \pi'(\rho\tau, \rho'\tau'; j) \exp(\mathrm{i}q\boldsymbol{R}_j). \tag{6}$$

A frequently used approximation to equation (6) is the local RMTA (LRMTA), neglecting all terms in the j sum over the unit cells, except for $j = 0$, and restricting to $\tau = \tau'$. Within the LRMTA the electronic part of equation (6) may be expressed through the phaseshifts, $\delta_l(\epsilon_{\mathrm{F}})$, and the matrix elements of $\mathrm{Im}\, g(\epsilon_{\mathrm{F}})$ with respect to the angular momentum quantum numbers (Gaspari and Gyorffy 1972). In the case of cubic symmetry the latter quantities may be expressed through the ratios of partial densities of states (DOS) and single-site partial DOS at ϵ_{F}, while in systems of lower point symmetry additional terms exist that will be worked out for the hexagonal structure in the present paper.

To treat λ_{spin}, we replace the phonon propagator D'' in equation (6) by $\mathrm{Im}\, \chi^{\mathrm{s}}_q(\rho\tau, \rho'\tau', \omega)$, the lattice Fourier transform of the imaginary part of the dynamical spin density correlation function and take into account that, due to the larger frequency extent of χ^{s}_q, the coupling function π^{s} is energy dependent. In the frame of the SDFA-RPA the electron–spin fluctuation coupling potential, K_{xc}, is the derivative of the exchange correlation potential V_{xc} with respect to the magnetization density. Collecting the relevant relations (Stenzel *et al* 1988), we obtain

$$\lambda_{\mathrm{spin}} = 2 \int \frac{\mathrm{d}\omega}{\omega} 3 \int \frac{\mathrm{d}q}{\Omega_{\mathrm{BZ}}} \alpha^2 F^{\mathrm{spin}}(q,\omega) \tag{7}$$

with

$$\alpha^2 F^{\mathrm{spin}}(q,\omega) = \sum_{\tau\tau'} \int \mathrm{d}\rho\, \mathrm{d}\rho' K_{\mathrm{xc}}(\rho,\tau) \pi^{\mathrm{s}}_q(\rho\tau, \rho'\tau'; \omega) \mathrm{Im}\, \chi^{\mathrm{s}}_q(\rho\tau, \rho'\tau'; \omega) K_{\mathrm{xc}}(\rho', \tau') \tag{8}$$

and

$$\pi^{\mathrm{s}}_q(\rho\tau, \rho'\tau'; \omega) = \frac{\omega}{\pi^3 n(\epsilon_{\mathrm{F}})} \int_{-\infty}^{\infty} \mathrm{d}x \left(\frac{f(x)}{(x - \omega - \epsilon_{\mathrm{F}})^2} + \frac{1 - f(x)}{(x + \omega - \epsilon_{\mathrm{F}})^2} \right)$$

$$\times \sum_j \exp(\mathrm{i}q\boldsymbol{R}_j) \mathrm{Im}\, g(\rho\tau, \rho'\tau'\boldsymbol{R}_j; \epsilon_{\mathrm{F}}) \mathrm{Im}\, g(\rho'\tau'\boldsymbol{R}_j, \rho\tau; x). \tag{9}$$

We evaluate χ^{s}_q by solving the following Bethe Salpeter equation:

$$\chi^{\mathrm{s}}_q(\rho\tau, \rho'\tau'; \omega) = \chi^{\mathrm{Ps}}_q(\rho\tau, \rho'\tau'; \omega) + \sum_{\tau_1} \int \mathrm{d}\rho_1 \chi^{\mathrm{Ps}}_q(\rho\tau, \rho_1\tau_1; \omega) K_{\mathrm{xc}}(\rho_1, \tau_1)$$

$$\times \chi^{\mathrm{s}}_q(\rho_1\tau_1, \rho'\tau'; \omega). \tag{10}$$

Here, χ^{Ps} is the non-interacting dynamical susceptibility. In the site–angular momentum representation χ^s_q reads

$$\chi^s_q = \sum_{\substack{LML'M'l_1l_2 \\ l'_1l'_2\kappa_1\kappa_2\kappa'_1\kappa'_2}} Y_{LM}(\rho) R^{\tau}_{l_1\kappa_1}(\rho) R^{\tau}_{l_2\kappa_2}(\rho) \hat{\chi}^s_q(LMl_1l_2\kappa_1\kappa_2; L'M'l'_1l'_2\kappa'_1\kappa'_2;\omega)$$

$$\times R^{\tau'}_{l'_1\kappa'_1}(\rho') R^{\tau'}_{l'_2\kappa'_2} Y_{L'M'}(\rho'). \tag{11}$$

Here, $R^{\tau}_{l\kappa}(\rho)$ is a ρ-dependent energy expansion coefficient of the radial part of the single-site electron wavefunction.

Introducing the matrix $\hat{\pi}^s_q$ similarly to $\hat{\chi}^s_q$, the expression for λ_{spin} in equation (8) may be written as the trace of a matrix product.

3. The bandstructure

Results of our scalar relativistic KKR bandstructure calculations for the hexagonal structure, using the exchange correlation potential of von Barth and Hedin (1972) are shown in figures 1 and 2. The Fermi energy falls into the lowest peak of the Sc d-band structure. We obtain $n(\epsilon_F) = 30.18$ states Ryd^{-1} atom^{-1} and for the partial DOS at ϵ_F: $n_0 = 0.497$, $n_1 = 7.64$, $n_2 = 21.38$, and $n_3 = 0.666$. Most important for the dynamical susceptibility is the 0.04 Ryd broad d DOS peak in the immediate vicinity of ϵ_F, but the structure 0.15 Ryd above the Fermi energy also has some influence on this quantity. The weak dispersion of the d bands for wavevectors in the q_z direction is also of great importance for χ^s, as a glance at figure 2 shows.

In comparison to the cubic case the point group of the hexagonal structure (D_{3h}) consists of one- and two-dimensional irreducible representations that can be partly built up by more than one specific angular momentum. (The representations and their bases for the D_{3h} local symmetry up to $l = 3$ are listed in table 1.) As a consequence, the on site one-particle Green function, $g^{\tau\tau',0}_{lm,l'm'}$, contains finite matrix elements that are diagonal in the angular momentum indices and therefore expressible through partial DOS and matrix elements that are not. Both kinds of matrix element, leading to important contributions to λ_{spin}, are displayed in table 2. For the phaseshifts at ϵ_F we obtain: $\delta_0 = -0.469$, $\delta_1 = -0.098$, $\delta_2 = 0.373$, and $\delta_3 = 0.0025$.

Table 1. Representations and their bases for D_{3h} local symmetry. Y_{lm} denotes real spherical harmonics. The representations are according to Bradley and Cracknell (1972).

Representation	Bases			
A'_1	Y_{00}		Y_{20}	Y_{3-3}
A'_2				Y_{33}
A''_2		Y_{10}		Y_{30}
E'		(Y_{11}, Y_{1-1})	(Y_{2-2}, Y_{22})	(Y_{31}, Y_{3-1})
E''			(Y_{21}, Y_{2-1})	(Y_{3-2}, Y_{32})

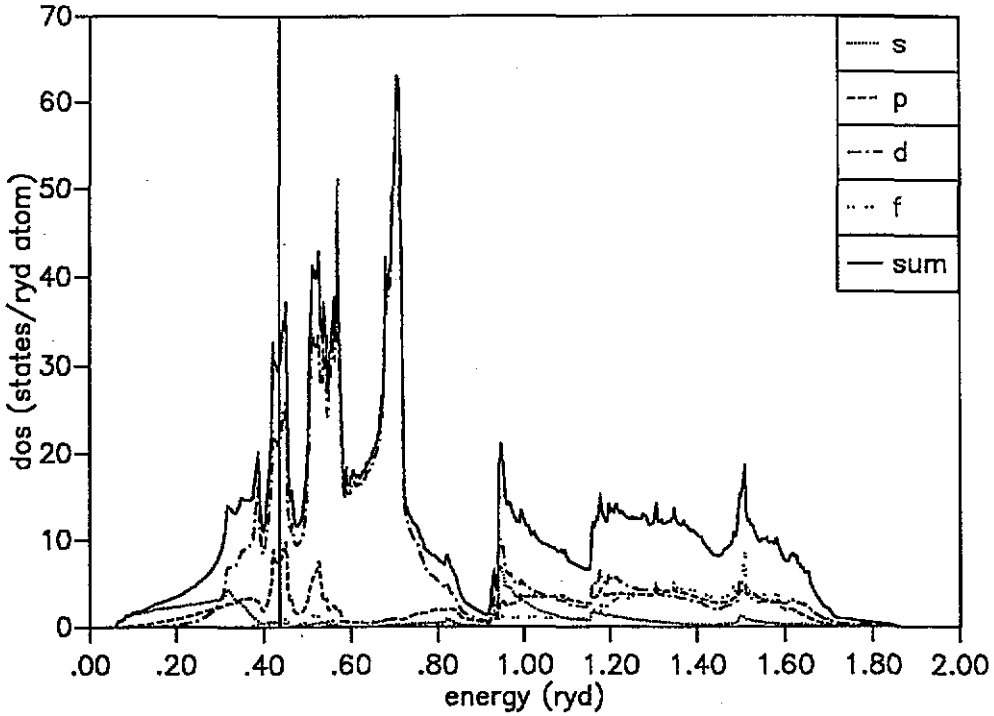

Figure 1. The s, p, d, and f partial DOS and the total DOS (sum) for Sc calculated for the 20 lowest valence bands. The vertical line at $\epsilon = 0.437$ Ryd designates the Fermi energy.

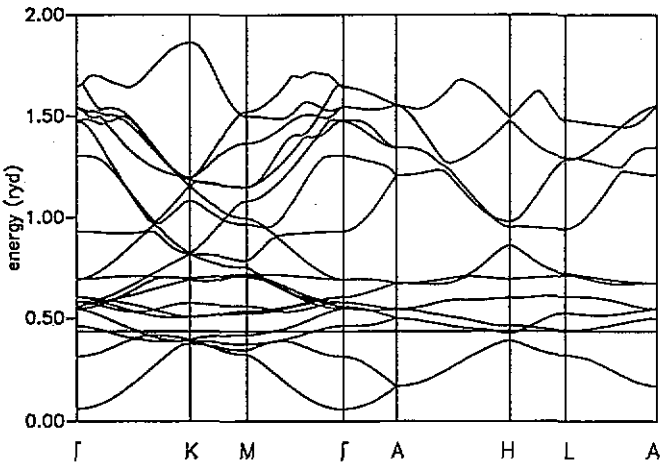

Figure 2. The lowest 20 valence bands of Sc along some symmetry directions within the IWBZ. The Fermi surface ($\epsilon_F = 0.437$ Ryd) is built up by bands 3 and 4.

4. Results

4.1. The phonon contribution

Due to a well known relation, derived by Gaspari and Gyorffy (1972), the matrix elements of the electron–phonon coupling potential between the radial parts of the single-site electron wavefunctions in equation (6) may be expressed through phaseshifts at ϵ_F. Introducing the symbols $n_l^{\tau 0}(\epsilon_F)$ for the single-site partial DOS, and

Table 2. The matrix elements, n_l^Γ, diagonal in angular momentum, and $\Omega_{l,l'}^\Gamma$, off-diagonal in angular momentum, of the on site one-particle Green function, $g_{lm,l'm'}^{\tau\tau',0}$, for the irreducible representations, Γ, of the D_{3h} point group. The values of n and Ω are defined by $n_l^\Gamma = (2/\pi)\sum_{m(\Gamma)} \mathrm{Im}\, g_{lm,lm}^{\tau\tau',0}$ and $\Omega_{l,l'}^\Gamma = (2/\pi)\sum_{m(\Gamma),m'(\Gamma)} \mathrm{Im}\, g_{lm,l'm'}^{\tau\tau',0}$, respectively. The numbers for the symmetry adapted DOS up to $l = 2$ given by Asada and Terakura (1982) are in states Ryd^{-1}/(atom spin dimension of the representation). They add up to a total DOS at ϵ_F of 29.80 states Ryd^{-1}/atom and thus lead to a lower value for λ than cited in the paper of Tsang *et al* (1985).

l		n_l^Γ	l		n_l^Γ	l	l'		$\Omega_{l,l'}^\Gamma$
0	A_1'	0.4969	3	A_2''	0.2735	0	2	A_1'	−0.2767
1	A_2''	2.0828	3	E'	0.0319	0	3	A_1'	−0.1608
1	E'	5.5569	3	E''	0.1168	2	3	A_1'	−0.6732
2	A_1'	6.9083				1	3	A_2''	−0.0345
2	E'	10.2074				1	2	E'	4.6993
2	E''	4.2618				1	3	E'	0.0573
3	A_1'	0.2353				2	3	E'	−0.2276
3	A_2'	0.0090				2	3	E''	−0.0569

the Gaunt numbers with respect to real spherical harmonics, G, we write equation (6) for the Eliashberg function in the following, more explicit form:

$$\alpha^2 F(\omega) = \frac{16\epsilon_F}{9\pi^2 n(\epsilon_F)} \sum_{j\tau\tau'} \frac{\mathrm{d}q}{\Omega_{BZ}} \exp[\mathrm{i}q(\tau - \tau' + R_j)] \frac{1}{\sqrt{M_\tau M_{\tau'}\omega}} \delta(\omega - \omega_{q,\lambda})$$
$$\times \sum_{MM'll_1l'l_1'} \frac{1}{(n_l^{\tau 0} n_{l_1}^{\tau 0} n_{l'}^{\tau' 0} n_{l_1'}^{\tau' 0})^{1/2}} \sin(\delta_l^\tau - \delta_{l_1}^\tau) \sin(\delta_{l'}^{\tau'} - \delta_{l_1'}^{\tau'})$$
$$\times (\delta_{l_1,l+1} - \delta_{l,l_1+1})(\delta_{l_1',l'+1} - \delta_{l',l_1'+1}) |e_{q,\lambda}^\tau||e_{q,\lambda}^{\tau'}| Y_{1M}(e_{q,\lambda}^\tau) Y_{1M'}(e_{q,\lambda}^{\tau'*})$$
$$\times \sum_{mm'm_1m_1'} G(1M, lm, l_1m_1) G(1M', l'm', l_1'm_1')$$
$$\times \mathrm{Im}\, g_{lml'm'}^{\tau\tau';j}(\epsilon_F) \mathrm{Im}\, g_{l_1m_1l_1'm_1'}^{\tau\tau';j}(\epsilon_F). \tag{12}$$

The cells j in equation (12) may be grouped into shells around the central cell ($j = 0$), whereby the coordinates R_j of a given shell are linked to each other by point group symmetry operations. As shown previously for a number of systems (Glötzel *et al* 1979), the j sum converges within a range of the order of 10 shells and in many cases even restriction to $j = 0$ and $\tau = \tau'$ (local approximation) yields sensible results. If we calculate the electronic quantity η, as defined by Gaspari and Gyorffy (1972), in local approximation, retaining only the terms expressible through partial DOS, we obtain: $\eta_1^{\mathrm{local}} = 2.14$ eV Å^{-2}, while inclusion of the other terms reduces it to 1.65 eV Å^{-2}. Using table 2 and equation (12) it is easy to write down the individual contributions to η.

In order to evaluate the Eliashberg function according to equation (12) we need to know the phonon spectrum. Figure 3 shows the phonon DOS, as obtained with the help of a Born–von Karman force constant model (Reichardt 1992) as fitted to the measured phonon dispersion curves of Pleschiutschnig *et al* (1991). The Eliashberg function resulting from the local approximation is shown in figure 4(*a*) (dotted curve). At small frequencies it is proportional to ω, leading to a finite value of the integrand

in equation (1) for λ_{phon} (dotted curve in figure 4(*b*)) at $\omega = 0$. The non-local function $\alpha^2 F$ on the other hand, evaluated by including 10 shells of cells (full curve of figure 4(*a*)), behaves nearly like ω^2 in the low-frequency regime and leads to a very small integrand in equation (12) (full curve in figure 4(*b*)) in the limit $\omega = 0$. The biggest differences between the integrands for the local approximation and the non-local treatment occur at frequencies up to 10 meV. We obtain $\lambda_{phon} = 0.470$. In the local approximation its value is 0.556.

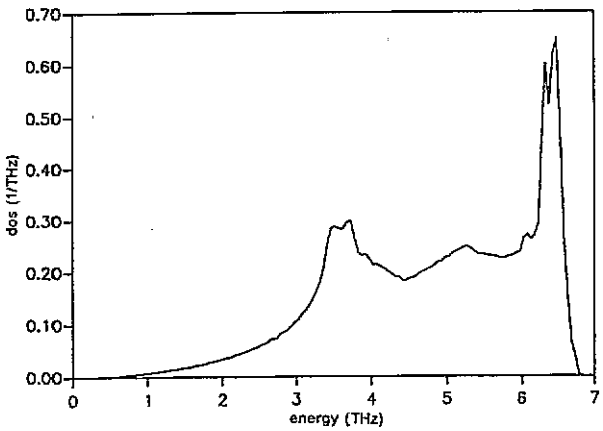

Figure 3. The phonon density of states of Sc as obtained by Pleschiutschnig *et al* (1991).

4.2. The spin fluctuation contribution

Using our KKR bandstructure data, we evaluated $\chi_q^{Ps}(\omega)$ and $\chi_q^s(\omega)$ for a number of q points in the irreducible wedge of the BZ (1WBZ). For illustrational purposes we discuss the spectral functions of the real space double Fourier transforms, $\mathrm{Im}\,\chi^s(q, q; \omega)$. As discussed in previous work (Götz and Winter 1993), χ^s of Sc depends considerably on the exchange correlation potential used to construct K_{xc}. This is in contrast to the bandstructure. We employed the potential according to Vosko *et al* (1980), since it leads to the best agreement between the experimental and the calculated total homogeneous low-temperature susceptibility (Götz and Winter 1993).

The amplitudes of $\mathrm{Im}\,\chi^{Ps}$ and $\mathrm{Im}\,\chi^s$ vary rapidly as a function of wavevector. Their low-frequency peaks at small q are due to intraband transitions within bands 3 and 4 crossing the Fermi level. On increasing wavevectors interband transitions within the high-DOS structure in the vicinity of 0.1 Ryd around ϵ_F come into play. Our susceptibility calculations concentrate on the q_x–q_z plane. The results for small q_x ($q_x = 0.05$ DU) are shown in figure 5(*a*). Intraband and for growing values of q_z also interband transitions near ϵ_F give rise to the low-energy peak, ranging to $\omega = 0.008$ Ryd at $q_z = 0$ and to $\omega = 0.03$ Ryd at the BZ boundary. Transitions into the higher-energy d band structures of the DOS show up only faintly in the susceptibility curves. The amplitudes of $\mathrm{Im}\,\chi^s$ increase for finite values of q_z and peak half way to the BZ boundary, where they are still substantially higher than at $q_z = 0$. The q-dependent Stoner enhancement parameter, $S(q)$ (table 3), behaves similarly, shooting up to a maximum value of 6.76 along this path. This property is due to the shallow dispersion of bands 3 and 4 in the q_z direction. Curves for $q_x = 0$ complete figure 5(*a*). In figure 5(*b*) we display some results for q vectors in the

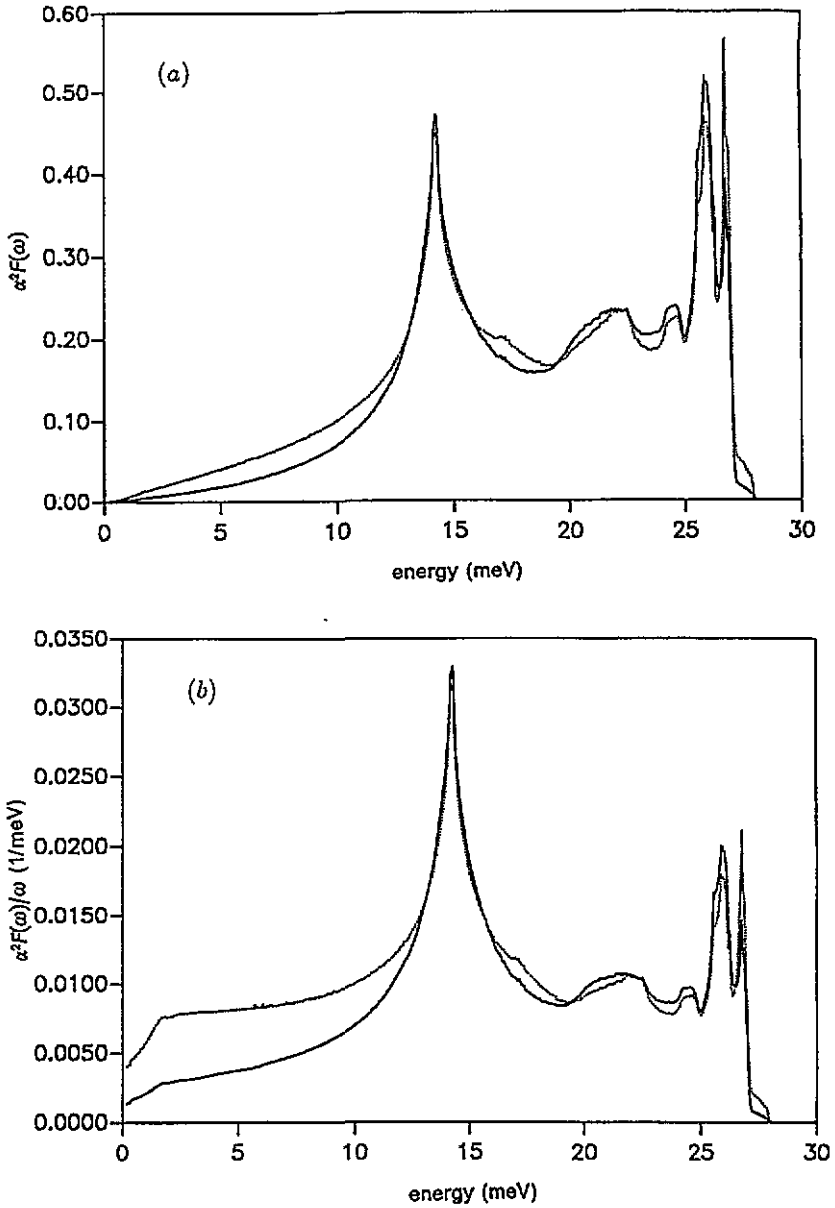

Figure 4. (*a*) The Eliashberg function $\alpha^2F(\omega)$ according to (12) taking into account 10 shells of cells (full curve). The dotted curve is the local approximation of $\alpha^2F(\omega)$. (*b*) Integrand of (1) to evaluate λ_{phon} obtained from the non-local (full curve) and the local (dotted curve) function $\alpha^2F(\omega)$.

q_x direction. On increasing q_x the amplitude of the low-frequency peak decreases, whereas a second peak due to transitions into the d-band structure around 0.15 Ryd above the Fermi energy builds up. Altogether, however, the magnitude of the spin fluctuations, including the Stoner enhancement, diminishes. The same observations can be made for the corresponding curves at $q_z = 0.15$ DU (figure 5(*c*)) and for q_z on the BZ boundary (figure 5(*d*)). In all cases the amplitudes at finite q_z exceed

those at $q_z = 0$. Curves obtained for $q = (0, 0.217, 0.313)$ are similar to those at $q = (0.25, 0, 0.313)$, exhibiting slightly larger amplitudes.

Table 3. Stoner enhancement factors, S, for several q points within the IWBZ. The values of q are in units of $2\pi/a$. $q_z^{BZ} = 0.3134$ DU.

q_x	q_y	q_z	$S(q)$	q_x	q_y	q_z	$S(q)$
0	0	0	3.66	0	0	0.15	6.76
0	0	q_z^{BZ}	4.79	0.05	0	0	2.87
0.05	0	0.15	6.09	0.05	0	q_z^{BZ}	6.34
0.25	0	0	2.54	0.25	0	0.15	3.16
0.25	0	q_z^{BZ}	3.68	0	0.217	q_z^{BZ}	4.02
0.50	0	0	1.89	0.50	0	0.15	2.08
0.50	0	q_z^{BZ}	1.70	2/3	0	0	1.72

The polarization functions $\pi^s(q, q; \omega)$, for the same wave vectors are collected in figure 6. The large values of this quantity are restricted to frequencies below 0.05 Ryd, limiting the important contributions of the spin fluctuations to λ_{spin} to the low-frequency regime. The amplitudes of π^s also decrease rapidly on growing wavevectors, an effect being counteracted by the increasing phase space weight. The curves for the q- and ω-dependent spin fluctuation Eliashberg functions, shown in figure 7, follow straightforwardly from equations (8) and (9) and figures 5 and 6.

To calculate λ_{spin} approximately, we evaluated the following integral over the q_x–q_z plane:

$$F_0 = 2\int_0^{q_{xBZ}} q_x \, dq_x \int_0^{q_{xBZ}} dq_z \int \frac{d\omega}{\omega} \alpha^2 F^{spin}(q, \omega) \Big/ \left(\int_0^{q_{xBZ}} q_x \, dq_x \int_0^{q_{xBZ}} dq_z \right). \tag{13}$$

Assuming approximate isotropy for this kind of integral with respect to the azimuthal angle ϕ within the BZ, we equate F_0 to λ_{spin} and obtain $\lambda_{spin} = 0.42$.

So both mechanisms together yield $\lambda = \lambda_{phon} + \lambda_{spin} = 0.89$, that has to be compared to $\lambda = 0.97$, a number resulting from the low-temperature specific heat measurements of Tsang *et al* (1985) and our calculated DOS at ϵ_F.

5. Summary

In this paper we have shown that the electronic contribution to the low-temperature specific heat of Sc can only be understood by treating both the phonon and the spin fluctuation contributions on the same footing. Our value for λ_{phon} lies between the number 0.3 deduced by Knapp and Jones (1972) through the extrapolation of high-temperature specific heat data on the one side and the theoretical number 0.64, as obtained by Papaconstantopoulos *et al* (1977) on the other side. Uncertainties in the Knapp–Jones value come from the fact that the high-temperature specific heat data show some scatter and that not only the phonon but also the spin fluctuation part depends on temperature. Furthermore, these authors use a model phonon DOS instead of the measured one. In contrast to Papaconstantopoulos *et al*, who treated Sc in a hypothetical BCC structure, our calculations have been performed for the real HCP structure, yielding an η value considerably below theirs. On the other hand, our

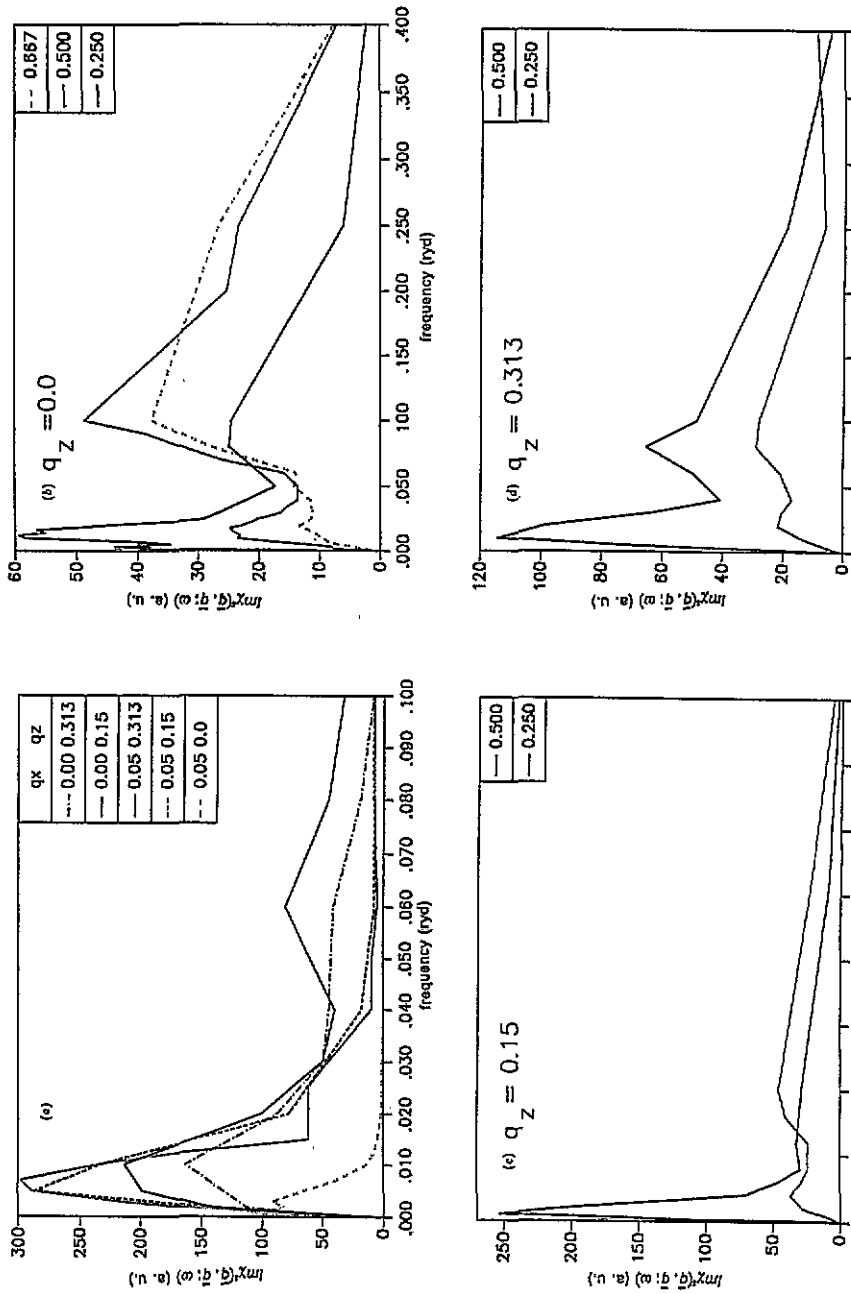

Figure 5. (*a*) The spectral function of the interacting spin susceptibility, Im $\chi(q, q; \omega)$, for some values of q with small values of q_z. (*b*) Im $\chi(q, q; \omega)$ for some values of q with $q_z = 0.0$. (*c*) Im $\chi(q, q; \omega)$ for $q = (0.25, 0.0, 0.15)$ DU and $q = (0.50, 0.0, 0.15)$ DU, respectively. (*d*) Im $\chi(q, q; \omega)$ for $q = (0.25, 0.0, 0.313)$ DU and $q = (0.50, 0.0, 0.313)$ DU, respectively.

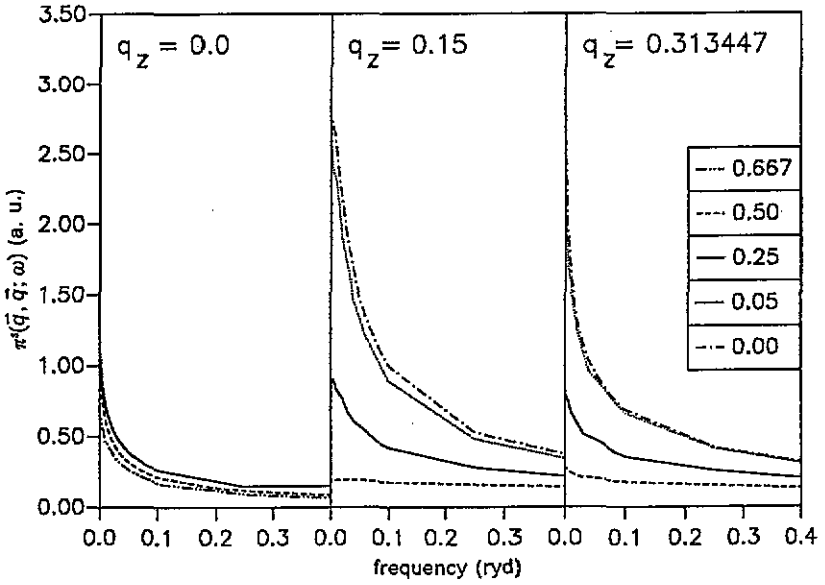

Figure 6. The electron–spin fluctuation coupling function, $\pi^s(q, q; \omega)$ for some values of q in the q_x–q_z plane.

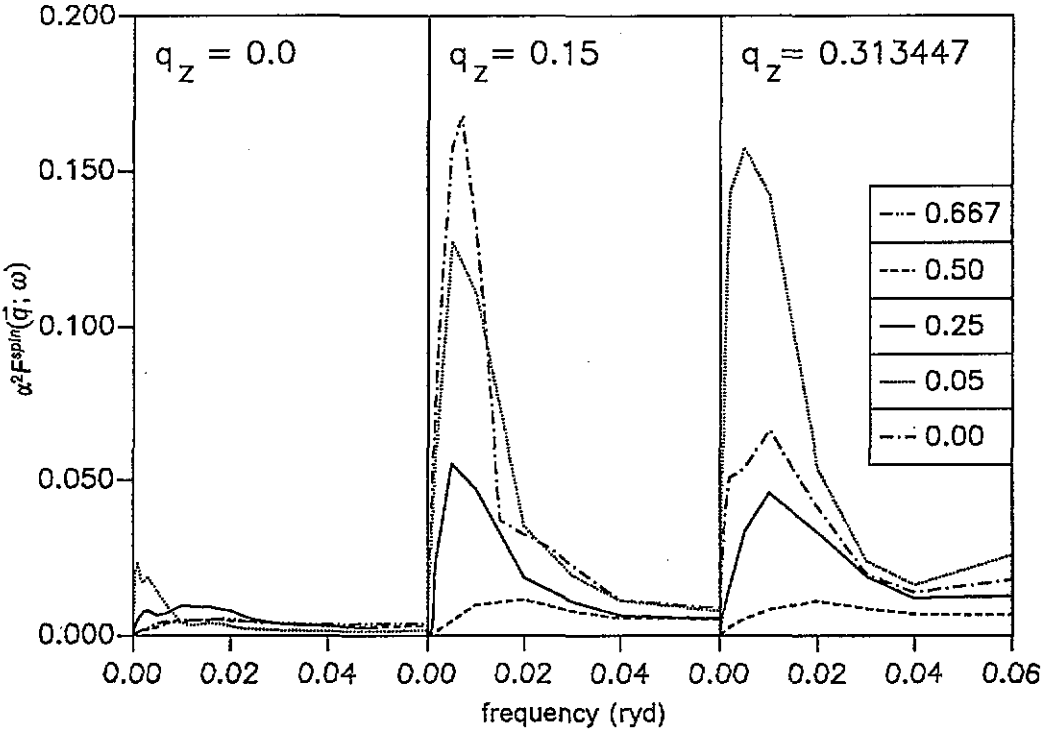

Figure 7. The spin fluctuation Eliashberg function, $\alpha^2 F^{\text{spin}}(q; \omega)$ for some values of q in the q_x–q_z plane.

use of the true phonon spectrum shows that the low-frequency transverse phonon modes enter the equation for λ_{phon} with a weight larger than accounted for by a theory expressing the phonons through some Debye frequency. As a consequence, our effective value for $1/\langle\omega^2\rangle$ in McMillan's formula (1968) exceeds that implied by Papaconstantopoulos *et al*, leading altogether to a sizeable number for λ_{phon}.

As expected from previous qualitative considerations, we found that the spin fluctuations yield a substantial contribution to λ. The spin fluctuation mass enhancement of Sc is in fact considerably larger than found for Pd (Stenzel *et al* 1988) that is being considered as the most prominent example for a highly Stoner enhanced paramagnetic elemental metal. The effect in Sc is so sizeable because in this substance χ^s has large amplitudes in a bigger portion of q space than in Pd. We have shown that χ^s of Sc is strongly wavevector dependent in the BZ and inclusion of more q points could somewhat change, probably somewhat increase, the calculated number for λ_{spin}. Some uncertainty concerning the exact value of λ_{spin} is also caused by the fact that χ^s depends non-negligibly on the exchange correlation potential chosen. To remove this uncertainty, evaluation of ground state energies for the partly spin polarized homogeneous electron gas in addition to calculations for fully spin polarized or paramagnetic systems would be highly desirable. Nonetheless, our *ab initio* results for the phonon and spin fluctuation Eliashberg functions and the electron mass enhancement are reasonably near to data deduced from experiment and calculated bandstructure DOS. Our results also give an understanding of why—in spite of a sizeable λ_{phon}—superconductivity is not observed in this system.

Acknowledgment

We thank Dr W Reichardt for useful discussions and for providing us with his computer program for the calculation of the phonon dispersion and the phonon density of states of Sc.

References

Asada T and Terakura K 1982 *J. Phys. F: Met. Phys.* **12** 1387
Bradley C J and Cracknell A P 1972 *The Mathematical Theory of Symmetry in Solids* (Oxford: Clarendon) p 66
Flotow H E and Osborne D W 1967 *Phys. Rev.* **160** 467
Gaspari G D and Gyorffy B L 1972 *Phys. Rev. Lett.* **28** 801
Glötzel D, Rainer D and Schober H R 1979 *Z. Phys.* B **35** 317
Gopta R P and Freeman A J 1976 *Phys. Rev. Lett.* **36** 613
Götz W and Winter H 1993 *J. Phys.: Condens. Matter* **5** 1707
Knapp G S and Jones R W 1972 *Phys. Rev.* B **6** 1761
McMillan W L 1968 *Phys. Rev.* **167** 331
Papaconstantopoulos D A, Boyer L L, Klein B M, Williams A R, Moruzzi V L and Janak J F 1977 *Phys. Rev.* B **15** 4221
Pleschiutschnig J, Blaschko O and Reichardt W 1991 *Phys. Rev.* B **44** 6794
Reichardt W 1992 private communication
Sen M and Chatterjee S 1980 *J. Phys. F: Met. Phys.* **10** 985
Stenzel E, Winter H, Szotek Z and Temmerman W M 1988 *Z. Phys.* B **70** 173
Tsang T-W E, Gschneidner K A Jr, Schmidt F A and Thome D K 1985 *Phys. Rev.* B **31** 235
Von Barth U and Hedin L 1972 *J. Phys. C: Solid State Phys.* **5** 1629
Vosko S H, Wilk L and Nusair M 1980 *Can. J. Phys.* **58** 1200